X-ray based micromechanical finite element modeling of composite materials

Mikkelsen, Lars Pilgaard; Emerson, Monica Jane; Jespersen, Kristine Munk; Dahl, Vedrana Andersen; Conradsen, Knut; Dahl, Anders Bjorholm

Published in:
Proceedings of 29th Nordic Seminar on Computational Mechanics

Publication date:
2016

Document Version
Publisher's PDF, also known as Version of record

29th Nordic Seminar on Computational Mechanics
NSCM-29
R. Larsson (Ed.)
2016

X-RAY BASED MICROMECHANICAL FINITE ELEMENT MODELING OF COMPOSITE MATERIALS

NSCM-29

LARS P. MIKKELSEN[*], MONICA J. EMERSON[†], KRISTINE M. JESPERSEN[*], VEDRANA A. DAHL[†], KNUT CONRADSEN[†], ANDERS B. DAHL[†]

[*] Composites and Materials Mechanics,
Department of Wind Energy
Technical University of Denmark
DTU Risø Campus, 4000 Roskilde, Denmark
e-mail: lapm@dtu.dk, web page: http://www.vindenergi.dtu.dk

[†] Image Analysis and Computer Graphics
Department of Applied Matematics and Computer Science
Technical University of Denmark
DTU Lyngby Campus, Building 324, 2800 Kgs. Lyngby, Denmark
e-mail: monj@dtu.dk, web page: http://www.compute.dtu.dk/

Key words: Non-crimp fabric, X-ray tomography, fiber segmentation, Multi-scale modeling.

Summary. This is a study of a uni-directional non-crimp fabric reinforced epoxy composite material typically used as the load carrying laminate in wind turbine blades. Based on a 3D x-ray tomography scan, the bundle and fibre/matrix structure of the composite is segmented. This segmentation is used in a multi-scale finite element model bridging the gap from the individual fibers organized in bundles to the stitched non-crimp fabric used for building up the load carrying laminates.

1 INTRODUCTION

The 3D x-ray tomography technique is an excellent tool for non-destructive studies of fiber reinforced composite materials. Nevertheless, bridging the gap between a volumetric image obtained from x-ray CT and a valid and geometrically accurate finite element model is not straightforward. The current study is addressing this using different segmentation techniques to extract the fiber and bundle structure from a specific non-crimp uni-directional glass fiber composite. The segmentation is used to identify the fibers as structural elements, defined by the position of the center lines, and to accurately assess the individual fiber diameters. The obtained quantities are validated against the actual tex values [g/km] of the fiber bundles used in the investigated non-crimp fabric. Subsequently, the obtained segmentation is transformed into a multiscale finite element model operating on both fiber and bundle scale. The finite element model is built using the scripting language Python and both the commercial finite element solver Abaqus and the “Computer Aided Learning of the Finite Element Method” CALFEM are used for solving the system. Regarding CALFEM, the work is based on a recently derived Python based version[1] of the program using the meshing tool GMSH[2]. To illustrate the principle in the multi-scale analysis, the present study is focusing on a 2D plane strain finite element based prediction of the transverse stiffness and Poisson's ratio of the fiber matrix system inside a fiber bundle and on the bundle structure using the extracted fiber properties. Nevertheless, the model can easily be extended to investigate effects such as e.g. the curing-induced residual stresses influencing the fatigue performance and the fiber orientation governed compression strength of composites used in the wind turbine industry.

2 MATERIAL SYSTEM

The material under study is a typical non-crimp glass fiber fabric reinforced epoxy composite used in wind turbines. . Below a small region of one ply is segmented and quantified. The ply is based on 2400 tex 0º rowings stitched to a thin backing layer consisting of ±45º and 90º 200 tex backing bundles. The 0º load carrying rowing is made of 17µm fibers while the backing is based on 16µm fibers. The mechanical properties of the constituents in the micromechanical model are reported later and consist of

- Glass fibers: $E_f = 80\,\text{GPa}$; $\nu_f = 0.2$; $\rho_f = 2.6\,\text{g/cm}^3$
- Epoxy matrix: $E_m = 3\,\text{GPa}$; $\nu_m = 0.4$; $\rho_m = 1.2\,\text{g/cm}^3$

A zoomed 3x3x3 mm^3 field of view (FoV) x-ray tomography scan of a test sample with a cross section of 15x4.5 mm^2 is performed. The resulting voxel size of the scan is 3µm. For more details on the x-ray tomography scan and the material system studies see Jespersen and Mikkelsen[3].

3 FIBRE SEGMENTATION

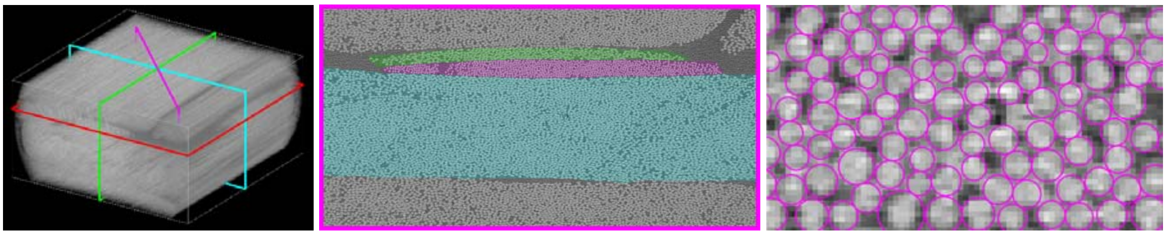

Figure 1: Cut planes for the bundle and fiber segmentation, a 45º bundle segmentation, and a close-up of a corresponding fiber segmentation. Cut planes, bundles and fibers are visualized in colors cyan: 0º, magenta: 45º and green: 90º

A complete 0º load carrying bundle as well as complete 90º and 45º bundles are contained in the 3x3x3mm^3 FoV scan. This makes it possible to choose three cut planes. Each cut plane is orthogonal to one of the bundles and contains its complete cross-section, as shown in Figure 1. All subsequent analysis is performed in those three 2D images, separately for each of the fiber bundles. The bundles are manually segmented, and the example of a 45º bundle is shown in Figure 1. For detecting the individual fibers, the automatic approach of Emerson et al.[4] is applied for estimating fiber centers. Fibers are then modeled as circles with the diameters calculated so that no fibers overlap, but all fibers touch at least one neighboring fiber. An example of the segmentation results for the fibers from a 45º bundle is shown in Figure 1.

In Table 1, the quantification of the individual bundles is presented where the 45º bundle actually includes two backing bundles. Compared with the expected fiber diameter of 17 μm and 16 μm for the load carrying 0º and the backing bundles (45º, 90º), respectively, the segmentation is found to under-estimate the diameters somehow. As it can be seen in the zoomed image in Figure 1, it is difficult to distinguish individual fibers, so some uncertainty may also be expected for the chosen resolution. The current segmentation is performed for 2D cross-sections and a full 3D based segmentation is expected to give an improved precision. Also, a scan with a higher zoom and a better resolution would improve the precision significantly. The last column in Table 1 shows the estimated tex-values based on the segmentated data. Compared with the tex-values reported for the fabric, the 0º load carrying bundle is found to be over-estimated while the backing bundles are found to be under-estimated. Based on the under-estimation of the fiber diameters, an under-estimation of the tex-values was expected for all the bundles. Nevertheless, the boundary between the load carrying 0º bundles can be hard to identify on a 2D slice, so the segmented results may include some part of a neighboring bundle.

Bundle	Number of fibers	Average fiber diameter	Total bundle area	Total fiber area	Local fiber volume fraction	Estimate tex-value
0º	5954	15.8μm	1.926mm^2	1.197mm^2	0.62	3113
45º	794	14.9μm	0.245mm^2	0.142mm^2	0.58	369
90º	375	15.4μm	0.125mm^2	0.071mm^2	0.57	185

Table 1 : Quantification from the fiber segmentation inside the bundles

3 MICROMECHANICAL MODEL

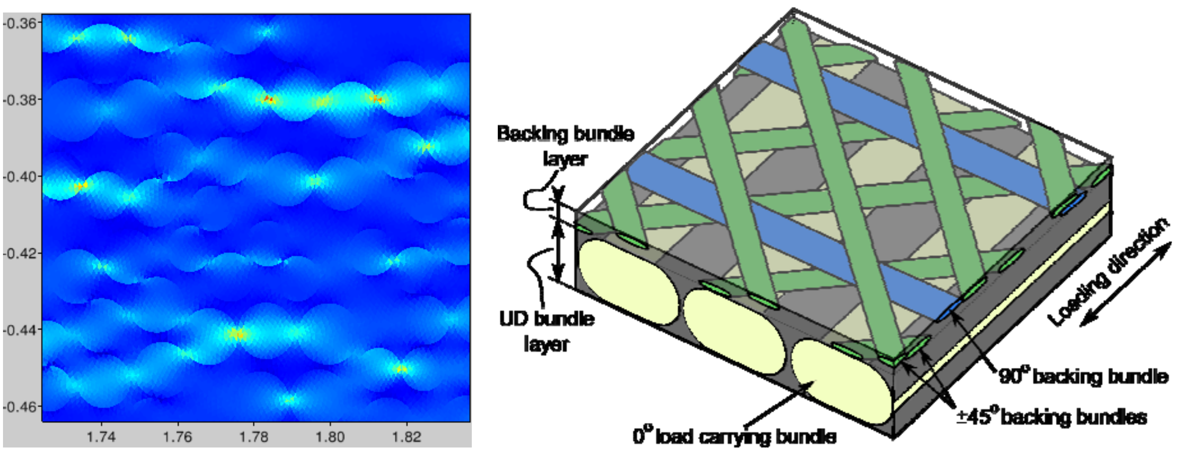

Figure 2: (a) The normal horizontal stress contour plot of a transverse loaded 45º backing bundle and (b) the 3D structure where the resulting constitutive law will be implemented

Based on the segmented fiber architecture, a 2-dimensional micromechanical model oriented orthogonally to the bundle orientation is built, see Figure 2a. In practice, the fiber architecture is segmented as fiber center points and diameters. Based on this, a representative rectangular part of the bundle area is selected for the finite element model and subsequently loaded in the transverse direction. As the much stiffer fibers will constrain the matrix deformation in the fiber direction, a plane strain linear triangle element is used. For the 45º bundle, a 1.0x0.1 mm^2 representative box with 443 fibers is selected. Only the solution for a very small part of 0.1x0.1mm^2 is shown in Figure 2a. The local fiber volume fraction inside the representative volume is found to be $V_f = 0.56$. Based on the micromechanical finite element model, the transverse stiffness and Poisson's ratio are found to be $E_{FEM} = 13.8\,\mathrm{GPa}$ and $\nu_{FEM} = 0.49$, whereas the inverse rules of mixture will give $E_{InvRoM} = 6.4\,\mathrm{GPa}$ and the Halpin-Tsai estimate will give $E_{Halpin-Tsai} = 11.8\,\mathrm{GPa}$. When the full 3D constitutive relation of the bundle structure is obtained, this will be applied on the segmented bundle structure which is sketched in Figure 2b.

4 DISCUSSION

A procedure for segmentation of the bundle structure and the fiber matrix structure inside the bundles is proposed. Based on this segmentation, an x-ray based micromechanical model is developed. For illustration, the transverse stiffness for the 45º bundles was estimated using the micromechanical model. In practice, all the stiffness parameters should be calculated in order to extract the full constitutive law of the bundle. Those constitutive laws for the different bundles can then be transformed into the overall bundle structure. Based on this multi-scale approach, it will be possible to estimate the stiffness properties of the laminates containing a large number of bundles and each of them containing thousands of fibers in turn. The multi-scale model is then used to estimate the drop in stiffness observed during fatigue failure under tension as well as to study the inter-fiber matrix stress stage during fatigue failure.

ACKNOWLEDGEMENTS

Financial support from CINEMA: "the allianCe for ImagiNg of Energy MAterials", DSF-grant no. 130500032B under "The Danish Council for Strategic Research" and from the European Union's Horizon 2020 research and innovation program under Grant Agreement No 685614, Bio4Selfis are gratefully acknowledged.

REFERENCES

[1] Lindemann, J. CALFEM for Python. https://github.com/CALFEM/calfem-python. (2015).

[2] Geuzaine, C. & Remacle, J. F. Gmsh: A 3-D finite element mesh generator with built-in pre- and post-processing facilities. *Int. J. Numer. Methods Eng.* **79,** 1309–1331 (2009).

[3] Jespersen, K. M. & Mikkelsen, L. P. Fatigue damage observed non-destructively in fibre composite coupon test specimens by X-ray CT. *IOP Conf. Ser. Mater. Sci. Eng.* **139,** 012024 (2016).

[4] Emerson, M. J., Jespersen, K. M., Jørgensen, P. S., Larsen, R. & Dahl, A. B. (2015, June). Dictionary based segmentation in volumes. In *Scandinavian Conference on Image Analysis* (pp. 504-515). Springer International Publishing.